Comparison of magnetic resonance imaging-based and conventional measurements for proton beam therapy of uveal melanoma

Jaarsma-Coes, M.G.; Ferreira, T.A.; Marinkovic, M.; Vu, T.H.K.; Vught, L. van; Haren, G.R.V.; ... ; Beenakker, J.W.M.

AMERICAN ACADEMY OF OPHTHALMOLOGY®

Comparison of Magnetic Resonance Imaging–Based and Conventional Measurements for Proton Beam Therapy of Uveal Melanoma

Myriam G. Jaarsma-Coes, MSc,[1,2] Teresa A. Ferreira, MD,[2] Marina Marinkovic, MD,[1] T.H. Khanh Vu, MD, PhD,[1] Luc van Vught, MSc,[1,2] Guido R. van Haren,[2] Myra F. Rodrigues, MD,[3,4] Yvonne L.B. Klaver, MD, PhD,[3,4] Berit M. Verbist, MD, PhD,[2,3] Gregorius P.M. Luyten, MD, PhD,[1] Coen R.N. Rasch, MD, PhD,[3,4] Jan-Willem M. Beenakker, PhD[1,2,4]

Objective: Conventionally, ocular proton therapy (PT) is planned using measurements obtained by an ophthalmologist using ultrasound, fundoscopy, biometry, and intraoperative assessments. Owing to the recent advances in magnetic resonance imaging (MRI) of uveal melanoma (UM), it is possible to acquire high-resolution 3-dimensional images of the eye, providing the opportunity to incorporate MRI in ocular PT planning. In this study, we described how these measurements can be obtained using MRI, compared the MRI-based measurements with conventional ophthalmic measurements, and identified potential pitfalls for both modalities.

Design: Cross-sectional study.

Subjects: Data from 23 consecutive patients with UM treated with PT were retrospectively evaluated.

Methods: Magnetic resonance imaging–based measurements of axial length, tumor height and basal diameter, and marker-tumor distances were compared with the conventional ophthalmic measurements, and discrepancies were evaluated in a multidisciplinary setting.

Main Outcome Measures: Tumor prominence and basal diameters on MRI and ultrasound, axial length on MRI and biometry, tumor-marker distances on MRI and measured intraoperatively.

Results: The mean absolute differences of the tumor height and basal diameter measurements between ultrasound and MRI were 0.57 mm and 1.44 mm, respectively. Larger absolute differences in height and basal diameter were observed when the full tumor extent was not visible on ultrasound (0.92 mm and 1.67 mm, respectively) compared with when the full tumor extent was visible (0.44 mm and 1.15 mm, respectively). When the full tumor was not visible on ultrasound, MRI was considered more reliable. Tumor-marker distances measured using MRI and intraoperative techniques differed < 1 mm in 55% of the markers. For anteriorly located and mushroom-shaped tumors (25% of the markers), MRI provided more accurate measurements. In flat UM (15% of the markers), however, it was difficult to delineate the tumor on MRI. The mean absolute difference in axial length between optical biometry and MRI was 0.50 mm. The presence of the tumor was found to influence optical biometry in 15 of 22 patients; the remaining patients showed a better agreement (0.30 mm). Magnetic resonance imaging–based biometry was considered more reliable in patients with UM.

Conclusions: Magnetic resonance imaging allowed for the 3-dimensional assessment of the tumor and surrounding tissue. In specific patients, it provided a more reliable measurement of axial length, tumor dimensions, and marker-tumor distances and could contribute to a more accurate treatment planning. Nevertheless, a combined evaluation remains advised, especially for flat UM. *Ophthalmology Retina 2023;7: 178-188 © 2022 by the American Academy of Ophthalmology. This is an open access article under the CC BY-NC-ND license (http://creativecommons.org/licenses/by-nc-nd/4.0/).*

Supplemental material available at www.ophthalmologyretina.org.

Uveal melanoma (UM) is the most common primary intraocular malignancy in adults, with an incidence of up to 14 cases per million person-years.[1,2] Proton therapy (PT), when available, is often the preferred treatment for larger UM and tumors that encircle the optic nerve. In the preparation for ocular PT, radiopaque (tantalum) markers are sutured to the sclera near the tumor border by an ophthalmologist for treatment planning and position verification during treatment.[3]

Currently, ocular PT is planned using a geometric tumor and eye model, based on data from different, mostly

https://doi.org/10.1016/j.oret.2022.06.019
ISSN 2468-6530/22

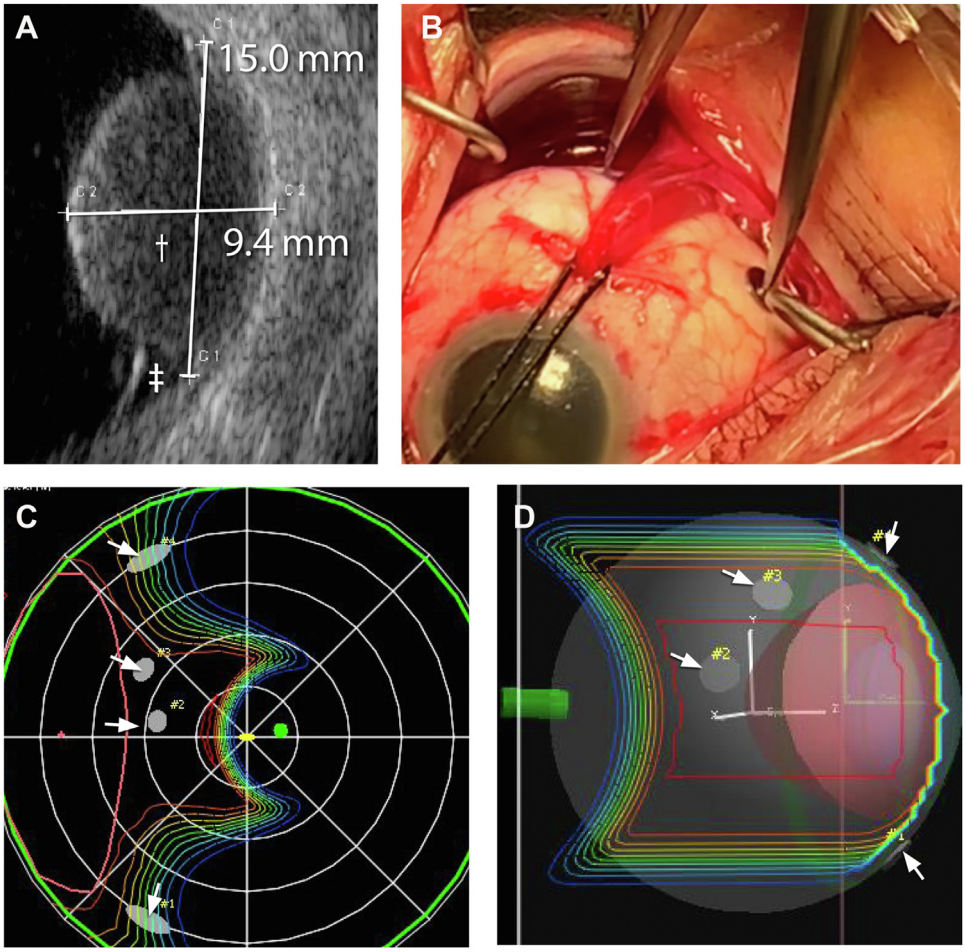

Figure 1. Ophthalmic measurements. **A,** Ultrasound-based measurements of tumor (dagger) prominence and basal diameter. Note the associated retinal detachment (double dagger). **B,** Intraoperatively, the distance between tumor and marker and distance between markers is measured using a caliper. **C, D,** Ocular proton therapy plan with the planned dose distribution. In the fundus view (**C**), the intraoperative and ultrasound-based measurements are used to define the tumor base, from which a geometric 3-dimensional model (**D**) of the eye, including the tumor (red) and markers (arrows), is constructed.

ophthalmic, sources such as ultrasound and fundoscopy (Fig 1).[4] In this model, the eye is scaled to the patient's axial length, as obtained by biometry. Additionally, the transversal diameter of the eye; combined thickness of the retina, choroid, and sclera; lens position and thickness; and limbus diameter can be personalized. The tumor geometry is primarily based on its height and basal diameters, as obtained from ocular ultrasound (Fig 1A), whereas intraoperatively obtained marker-tumor distances and fundus photographs are used to define the tumor base (Fig 1B).

Although this approach results in high rates of $>$ 95% of local control,[3,5] this comes at the cost of a significant reduction of visual acuity, approximately 45% of the eyes losing $>$ 3 Snellen lines in 10 years.[6–8] Part of this vision loss can be attributed to the relatively large safety margins of up to 3 mm,[5] which are required to mitigate different uncertainties in treatment planning and delivery, including uncertainties in tumor geometry and location.

Ocular magnetic resonance imaging (MRI) has become a valuable tool in the diagnosis, therapy selection, and follow-up of patients with UM.[9–12] Similarly, for malignancies in other body parts, MRI has the potential to reduce uncertainties in ocular PT and thereby contribute to strategies to reduce the radiation-induced side effects.[13] In particular, MRI could potentially provide valuable information for current treatment, model based, planning as it provides the following: (1) 3-dimensional (3D) visualization of the tumor and its surrounding structures[3,14,15]; (2) tumor and globe dimensions, including transversal diameter, which cannot be measured using ophthalmic imaging techniques[15–18]; and (3) depiction of the surgical markers in relation to tumor and eye.[19]

In this study, we described and evaluated a dedicated MRI protocol to obtain the geometric measurements that can be used to complement conventional measurements for ocular PT planning. We compared MRI-based measurements with conventional ophthalmic measurements of the axial eye length, height and the largest basal diameter (LBD) of the tumor, and marker-tumor distances and identified potential pitfalls for both conventional and MRI-based measurements.

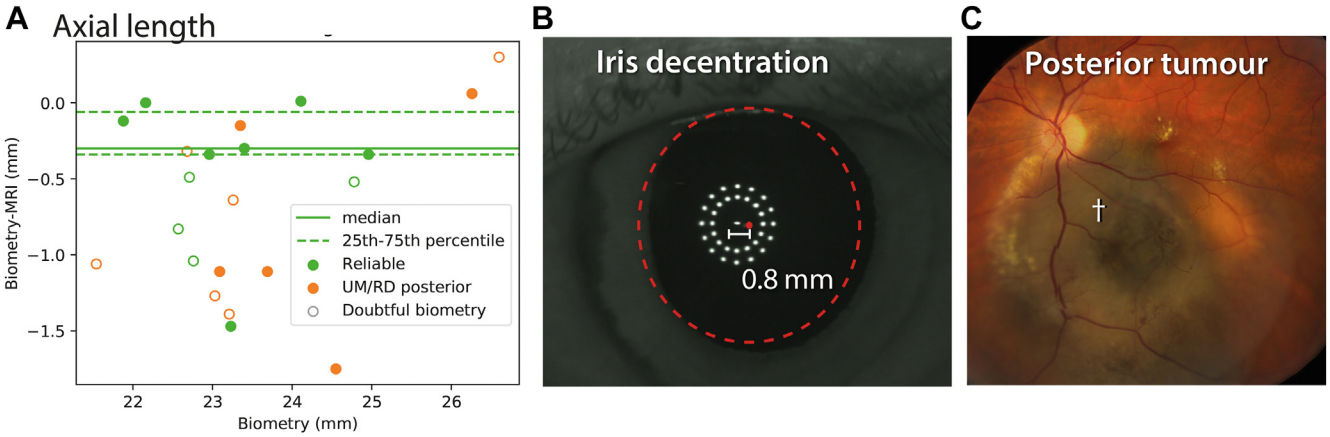

Figure 2. A, Difference between magnetic resonance imaging (MRI)-based and biometry-based eye length measurements. For all patients including doubtful biometry (open dots) and patients with a uveal melanoma (UM) or retinal detachment in the posterior pole (orange dots), on average, 0.6-mm shorter measurements were found. For the remaining patients (filled green dots), there was generally a good agreement between both techniques, except for 1 patient in whom part of the sclera was included in the MRI-based measurement **B, C,** Two examples of doubtful biometry measures: **B,** A large iris decentration is a sign that the measurement was not obtained along the optical axis; **C,** As the UM is covering the macula, the biometer reports a too short axial length.

Methods

Clinical data of 23 consecutive patients with UM, diagnosed by an ocular oncologist between December 2019 and October 2020 and treated with ocular PT, were evaluated retrospectively. Patients were referred to HollandPTC (Delft, the Netherlands) for ocular PT if UM was located juxtapapillary (26%) or when the tumor dimensions exceeded the local criteria for ruthenium plaque brachytherapy (height including sclera $>$ 7 mm or basal diameter $>$ 16 mm) (74%).[20,21] Patients underwent diagnostic MRI on a 3T MRI scanner (Ingenia Elition; Philips Healthcare), as part of clinical care, to confirm eligibility and localize the tumor in 3 dimensions (a detailed description is provided in the "MRI" section of Methods). Additionally, second, shorter MRI is performed 7 to 14 days after the placement of the markers to determine the tumor-marker distances. The study was conducted according to the guidelines of the Declaration of Helsinki and approved by the Ethics Committee Medisch Ethische Toetsings Commissie (METC) Leiden Den Haag Delft (G20.16; January 4, 2021). Informed consent for the retrospective use of their clinical data was obtained from all participants.

Conventional Measurements for Treatment Planning

The axial length of the affected eye in millimeters was obtained using optical biometry (Lenstar LS900, Eyesuite biometry, version 2.7.1; Haag-Streit) performed by an optometrist. Three aspects were evaluated for the affected eye: (1) the extended outputs of the biometer for signs of an unreliable measurement[22]; (2) the iris decentration, as an objective test of whether the measurement was performed along the visual axis[23]; and (3) presence of tumor or retinal detachment in the posterior pole. Further details are described in Figure 2 and Appendix S1 (available at www.ophthalmologyretina.org).

Tumor size was measured using ocular B-mode ultrasound (Aviso; Quantel Medical) as part of clinical care by their ophthalmologist. For patients with an anteriorly located tumor, additional images were acquired using an ultrasound biomicroscopy probe. To obtain tumor height, the distance of the highest point of the tumor to sclera was measured perpendicular to the scleral surface. The sclera was included for reliable, consistent measurements. The LBD of the tumor was then obtained, and the second diameter was defined as the largest diameter perpendicular to this measurement. All ultrasound images were retrospectively evaluated by an ocular oncologist (T.K.H.V.) and a physicist (J-W.M.B.) to assess whether the complete tumor base and apex were visible (Fig 3). Final scores were based on consensus.

After the placement of the markers, the distance between the center of the markers and the edge of the tumor (marker-tumor distances) was measured intraoperatively for each marker using a caliper. Simulations of transpupillary illumination measurements were performed using ray tracing, as developed by van Vught et al,[24] for 1 representative patient (details can be found in Appendix S2, available at www.ophthalmologyretina.org) to assess how the tumor blocks part of the light rays, introducing a penumbra.

Magnetic Resonance Imaging

Magnetic resonance imaging was performed as described by Ferreira et al.[10] In short, a 4.7-cm surface receive coil (Philips Healthcare) was used to image the affected eye. A radiotherapy head support was used for patient fixation. The MRI protocols are summarized below and in Table 1. A more detailed description, including planning of the scans, can be found in Appendix S3 (available at www.ophthalmologyretina.org).

The MRI scan obtained before marker surgery was used for baseline evaluation of the UM and measurements of the tumor and eye geometry. The protocol included 3D isotropic volumetric scans to assess the tumor and eye geometry, 2-dimensional (2D) scans to evaluate tumor origin and extension, and functional scans to assess the tumor diffusivity and perfusion.[10,15]

After surgery, second MRI was performed to assess the markers-tumor relation. These scans were acquired with stronger gradients and localized shimming to limit the signal voids caused by the susceptibility artifacts of the tantalum markers. The 3D isotropic volumetric scans were acquired for marker localization and comparison with preoperative MRI. Additionally, for each marker, gradient echo T1-weighted and spin echo T2-weighted 2D scans, perpendicular to the tumor base, were acquired (Fig 4D).

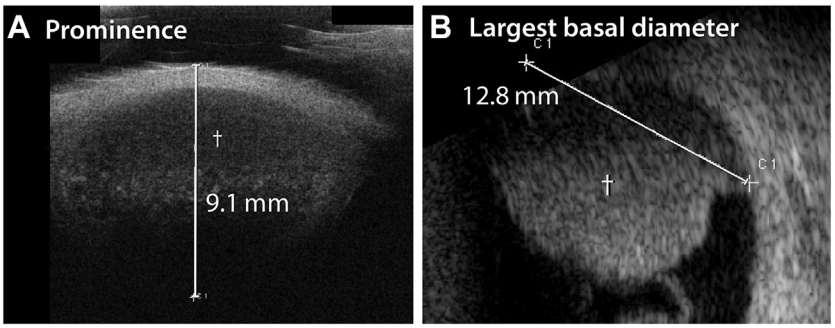

Figure 3. On ocular ultrasound, the full extent of the tumor (dagger) cannot always be visualized owing to its limited penetration depth (**A**) or field of view (**B**). These measurements were marked as unreliable and analyzed separately.

Evaluation of the Presurgery MRI Scans

All MRI images were evaluated by one of the neuroradiologists (B.M.V., T.A.F.) specialized in the eye at our center using Sectra IDS7 (version 21.1, Sectra AB). In case of doubt, a second reader evaluated the scans, and the final measurements were based on consensus. First, an evaluation of the tumor was performed, including screening for extrascleral extension and invasion of the ciliary body or optic nerve.[15] Additionally, both functional scans were assessed to confirm that the lesion matched the general characteristics of UM and to provide a baseline for the follow-up after PT.[15]

Subsequently, PT-specific measurements were obtained. The axial length of the eye, measured from the anterior wall of the cornea until the posterior wall of the retina, was preferably obtained from the 3D T2-weighted scans because, on T2-weighted sequences, the cornea is generally better depicted than on T1-weighted sequences. Because the optical or visual axis cannot be directly obtained from MRI scans,[25] the axial length was measured perpendicular to the lens plane and through the center of the lens or pupil (Fig 4A). The transversal diameter of the eye was obtained in the same plane perpendicular to the eye length, and it includes the sclera thickness bilaterally. The combined thickness of the sclera, choroid, and retina was measured on the contrast-enhanced multislice T1-weighted scan, as it provides a high in-plane resolution and good contrast among the sclera, choroid/retina, and vitreous body.

Tumor height and the largest and second basal diameter were primarily measured on contrast-enhanced 3D T1-weighted images (Fig 4B, C), as its isotropic resolution allowed for multiplanar reconstructions (Fig 4F), enabling measurements of the tumor dimensions in every possible direction, and because, on these images, the tumor is well differentiated from the retinal detachment. Moreover, the outer limit of the sclera can clearly be identified on these images.[10] When severe motion artifacts were present or in case of retinal detachment obscuring delineation between tumor and retinal detachment, the 3D T2-weighted or the contrast-enhanced 2D T1-weighted images were used. To allow comparison between ultrasound-based and MRI-based measurements, tumor height was measured including the sclera. For the PT planning, the sclera thickness was later subtracted.

Evaluation of the Postsurgery MRI Scans

Tumor dimensions and retinal detachment were compared with the presurgery images to ensure that no significant tumor growth or increase of the retinal detachment had occurred. Additionally, fat-suppressed T2-weighted images were evaluated for the presence of substantial inflammatory reactions that could have been induced by the surgery.

For each marker, the shortest distance between the tumor base and marker edge (marker-tumor distance) was measured (Fig 4E). For some mushroom-shaped tumors, an additional measurement was obtained from the marker to the projection of the overhanging intraocular tumor component on the sclera. This measurement was used to ensure that the entire tumor was incorporated in the radiation field because the treatment planning system used, Eclipse Ocular Proton Planning (Varian Medical Systems), cannot incorporate a mushroom geometry.

Comparison between the Ophthalmic and MRI-Derived Measurements

Optical biometry, ultrasound, and intraoperative marker-tumor distance measurements were compared with MRI-based measurements. Differences exceeding 0.5 mm for height and 1.0 mm for the other measurements were evaluated in a multidisciplinary setting with an ophthalmologist (M.M.), radiologist (B.M.V. and, T.A.F.), radiation oncologist (C.R.N.R.), and physicist (J-W.M.B). A paired *t* test was used to test for systematic differences between ophthalmic and MRI-derived measurements. Additionally, the interquartile range (IQR; 25th and 75th percentile) was determined.

Results

In 11 (48%) of the 23 cases, UM was in the right eye. According to the American Joint Committee on Cancer (eighth edition),[26] tumor classes ranged from T1 to T4, although the majority (65%) of the tumors were classified as stage T3. Five lesions were characterized as (partly) flat by the ophthalmologist on the basis of fundoscopy and ultrasound. In the majority of the patients, 4 tantalum markers (Altomed) were sutured on the outside of the sclera. In 1 patient, however, only 3 markers were used; in another patient, 5 markers were used. The time between the 2 MRI scans was on average 19 days (range, 7–49 days). No change in the tumor geometry had been observed, only an increase in retinal detachment. The differences and potential source of the discrepancies between conventional and MRI-based measurements are reported below. A detailed description of each patient can be found in Appendix S4 (available at www.ophthalmologyretina.org).

Table 1. Scan Parameters

Purpose	Scan Name	Voxel Size (mm^3)	TE (msec)/TR (msec)/Flip or Reference Angle (°)	Scan Time (mm:ss)	Additional Parameters
Preoperative scan					
3D measurements	3DT1 TSE	0.8 × 0.8 × 0.8	26/400/90	02:07	
	3DT1 TSE SPIR	0.8 × 0.8 × 0.8	26/400/90	02:07	
	3DT1 TSE SPIR gd	0.8 × 0.8 × 0.8	26/400/90	02:07	
	3DT2 TSE SPIR	0.8 × 0.8 × 0.8	305/2500/35	02:58	
Tumor origin and extension	MST1 TSE	0.5 × 0.5 × 2	8.0/400/90	00:43	
	MST1 TSE SPIR gd	0.5 × 0.5 × 2	8.0/400/90	00:43	
	MST2 TSE	0.4 × 0.4 × 2	90/2256/90	01:08	
Functional scans	DWI (TSE)	1.3 × 1.4 × 2.4	50/1555/50	1:33	B = 0, 800 sec/mm^2
	DCE	1.3 × 1.5 × 1.5	2.3/4.5/13	4:00	2 sec/dynamic
Postoperative scan					
Marker localization, tumor base localization, and comparison presurgery images	3DT1 GE	0.9 × 0.9 × 0.9	2.0/7.0/9	00:43	BW = 812 Hz
	3DT1 TSE	0.8 × 0.8 × 0.8	27/400/90	02:07	BW = 758 Hz
	3DT2 TSE	0.8 × 0.8 × 0.8	294/2300/35	02:43	BW = 943 Hz
	MST1 GE *gd**	0.6 × 0.6 × 2	2.8/7.0/9	00:33	BW = 532 Hz
	3DT1 TSE gd†	*0.8 × 0.8 × 0.8*	*25/400/90*	*02:07*	*BW = 758 Hz*
Marker-tumor distance	MST2 TSE *gd**	0.4 × 0.4 × 2	90/943/90	01:04	BW = 354 Hz
	MST1 GE *gd**	0.6 × 0.6 × 2	2.8/7/9	00:25	BW = 532 Hz
	MST1 TSE gd†	*0.5 × 0.5 × 2*	*6.0/718/90*	*00:43*	*BW = 658 Hz*
Check for motion	MST1 GE gd*	0.6 × 0.6 × 2	2.8/7.0/9	00:33	BW = 532 Hz
Screen for inflammation	3DT2 TSE SPIR *gd**	0.8 × 0.8 × 0.8	297/2300/35	02:43	BW = 943 Hz

3D = 3-dimensional; B = b-value (degree of diffusion weighting); BW = bandwidth; DCE = dynamic contrast-enhanced scan; DWI = diffusion-weighted imaging; gd = gadolinium; GE = gradient echo; MS = multislice; SPIR = spectral presaturation with inversion recovery; TE = echo time; TR = repletion time; TSE = turbo spin echo.
Although the patients in this study did not receive a contrast agent for the postoperative magnetic resonance imaging, we advise to perform the postoperative scans with contrast to aid in the differentiation between tumor and retinal detachment. Italic values indicate scans that were not performed within this study.
*These scans were performed without a contrast agent.
†These scans were not performed in this study.

Eye Geometry

Magnetic resonance imaging reported on average a longer axial length than that reported using biometry (IQR, −1.10 mm to −0.19 mm; $P < 0.001$) and a mean absolute difference of 0.66 mm (Fig 2A). In 8 patients, the difference between MRI-based and biometry measurements exceeded 1.0 mm. In the majority of these patients (75%, n = 6), the tumor or retinal detachment was present in the posterior pole, and the biometry showed signs of an unreliable measurement (50%, n = 4). In 1 patient, the MRI-based measurement was found to be incorrect because the sclera was included in the measurement (Appendix S1 [Fig A1, part D]). However, in 15 of 22 eyes, the extended evaluation of the biometry output showed signs of a potential inaccurate measurement, such as a large iris decentration. In these patients, a larger mean absolute difference of 0.8 mm (IQR of the difference, −1.1 mm to −0.4 mm) was observed than in the remaining 7 patients with unaffected measurement of 0.3 mm (IQR of the difference, −0.34 mm to −0.06 mm) (Fig 2A, B; Appendix S1).

Tumor Geometry

There was no overall significant difference between MRI-based and ultrasound-based tumor height measurements (IQR, −0.4 mm to 0.5 mm; $P = 0.75$; Fig 5A, C). The measurements had a mean absolute difference of 0.57 mm. In 6 patients, the tumor apex was not visible on the ultrasound images. These patients showed a larger absolute difference between MRI and ultrasound than the remaining patients where the tumor apex was visible (0.92 mm versus 0.44 mm, respectively). In 10 patients, the difference between ultrasound and MRI exceeded 0.5 mm. In 50% of these patients, the tumor apex was not visible on ultrasound, and the multidisciplinary tumor board considered MRI more reliable for these patients. Remaining differences exceeding 0.5 mm were found in flat melanomas or oblique-oriented tumors with a complex shape (Fig 5C). A more extensive description of the individual cases can be found in Appendix S4.

There was no significant difference between the average of all 23 MRI and ultrasound-based LBD measurements (IQR: −0.95 to 1.35 mm, $P = 0.39$; Fig 5B, D). The measurements had a mean absolute difference of 1.44 mm. In 14 patients, the difference between ultrasound and MRI exceeded 1 mm. In 8 (57%) of these patients, the full extent of the tumor base was not visible on ultrasound, and as a result, MRI was considered more reliable. In 3 patients with a flat melanoma, there was uncertainty about the accuracy of the MRI-based measurement. In 1 patient, a hyperintense enhancing region adjacent to the tumor was included on ultrasound but not included in the basal diameter

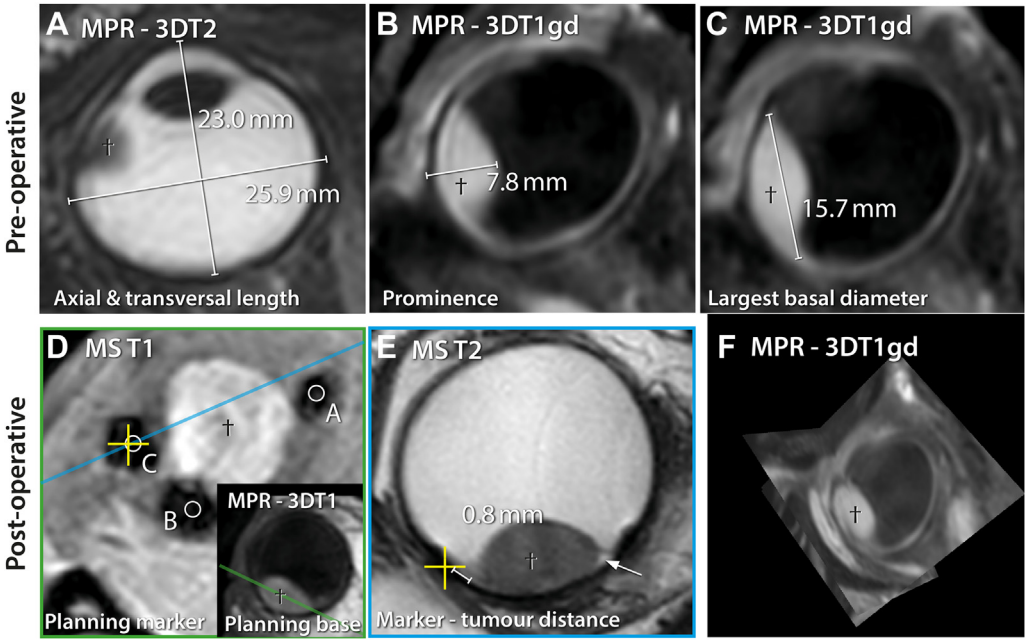

Figure 4. Primary preoperative and postoperative magnetic resonance imaging–based measurements. **A,** The axial length and transversal length were measured on a multiplanar reconstruction of the 3-dimensional (3D) T2-weighted scan. **B, C,** The prominence, including sclera, and largest basal diameter were measured on a multiplanar reconstruction of the 3D T1-weighted gadolinium scan. **D,** A multislice T1-weighted scan was acquired through the base of the tumor (dagger). Subsequent scans per marker (T2 [**E**] and T1) were acquired perpendicular to this plane through the center of the tumor and marker. **E,** Multislice T2-weighted scan is used to measure the distance between tumor and marker. Note the small retinal detachment adjacent to the uveal melanoma (arrow). **F,** Three-dimensional volumes as acquired with magnetic resonance imaging allow for multiplanar reconstruction in all directions, providing the opportunity to accurately determine the largest basal diameter and prominence and visualize the relation between tumor and surrounding tissue. MRI = magnetic resonance imaging; RD = retinal detachment; UM = uveal melanoma.

on MRI (Fig 5D). Similarly, in 1 patient, choroidal thickening adjacent to the tumor was not included in the MRI-based measurement, whereas it was included in the ultrasound-based measurement. For the 9 patients in whom the complete tumor base was visible on ultrasound (Fig 3), the mean absolute difference was 1.15 mm (IQR of the difference, 0.70–1.40 mm), compared with 1.67 mm (IQR, −1.80 mm to 1.30 mm) when the tumor base was not completely visualized. Similar results were found for the second basal diameter measurement, with a median absolute difference of 0.7 mm (IQR of the difference, −0.43 mm to 1.33 mm) for 13 patients with the entire tumor in the field of view.

Marker-Tumor Distances

In 1 patient, 1 of the marker-tumor distances could not be measured intraoperatively. Magnetic resonance imaging reported on average larger marker-tumor distances than that reported using intraoperative measurements (Fig 6; mean difference, 1.2 mm; $P < 0.01$). For 39 of the 87 (45%) evaluated markers, the difference between both measurements exceeded 1 mm. Magnetic resonance imaging showed a larger marker-tumor distance for the majority of these markers (n = 30). The multidisciplinary evaluation of markers with a difference exceeding 1 mm revealed 4 primary reasons for these differences. First, differences were found in 13 of the 18 markers in patients with flat melanomas. For these tumors, the extent was difficult to assess on MRI, and the intraoperative measurements were generally considered more reliable. Second, differences were found in 13 markers with a complex marker-tumor relation (Fig 6A–D). For markers located far from the tumor and in case of mushroom-shaped tumors, the marker-tumor distance could not easily be captured in a simple 1-dimensional distance measurement, which likely accounts for the observed differences between both modalities. Third, for anteriorly located tumors, the shadow cast during transillumination could cause an overestimation of the tumor extent for a posteriorly located marker (9 markers; Fig 6E). Personalized optical ray tracing simulations confirmed this shadow and showed that, for this specific patient, the shadow extended until the location of the markers, matching the intraoperative marker-tumor measurements. Finally, in 2 patients, the intraoperative annotation of 2 markers seemed to have been interchanged.

Discussion

In ocular PT, geometric information from different, mostly ophthalmic, sources are combined to construct a model of the tumor and eye for treatment planning.[4,12] In this study, we compared MRI-based and conventional measurements used to construct such a model and showed that, in specific conditions, MRI can improve the accuracy of this model. In line with earlier studies by Daftari et al,[27] Marnitz et al,[28] and Via et al,[29] this improved accuracy can contribute to strategies to reduce the irradiated volume and thereby reduce the radiation-induced side effects.

A general benefit of MRI was that 3D information of tumor, markers, and surrounding anatomy is available to all specialists involved in the treatment and can be used to

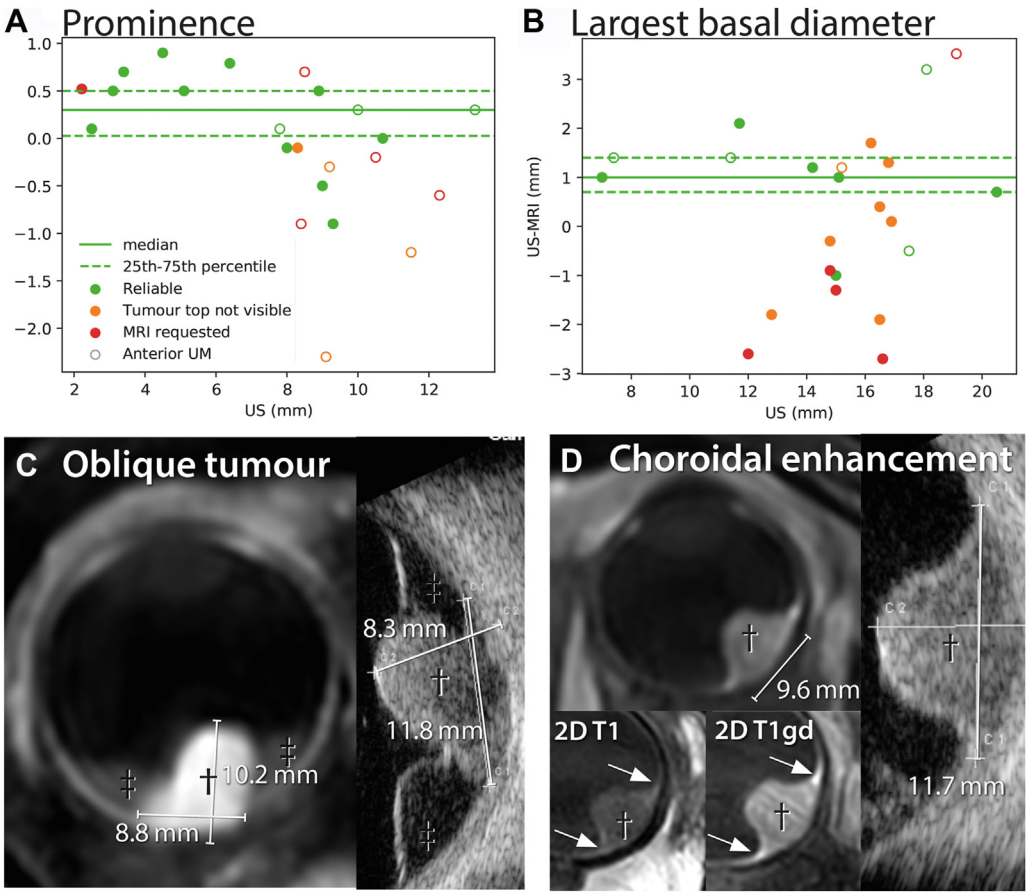

Figure 5. Comparison between ultrasound (US)-based and magnetic resonance imaging (MRI)-based measurements of the tumor geometry. **A,** For 5 patients (red), an MRI scan was requested because of doubts on the accuracy of the US-based measurements. Additionally, 7 US-based measurements were scored as potentially inaccurate (orange), as they did not show the complete tumor in the field of view. Notably, for 10 of these 12 patients, the tumor was located anteriorly (open markers). Overall, the largest differences were observed in anterior uveal melanoma (UM). **B,** For the patients with an reliable US-based measurement, an average absolute difference between both techniques of 1.2 mm for the largest and 1.6 mm for the second basal diameter was found. Overall, the largest differences were observed in unreliable US-based measurements. **C,** Prominence measurements for oblique-oriented tumors are not well defined and can differ between observers on both US and MRI. **D,** On MRI, choroidal enhancement was not included in the basal diameter measurements. On US, however, this seems to be included. gd = gadolinium.

evaluate the full 3D geometry of the tumor. For example, using MRI, the relation between tumor and markers can be visualized in 3 dimensions, whereas, conventionally, only a 2D projection is available (Fig 6E; Appendix S2). In this context, the multiplanar reconstructions proved to be beneficial to translate the clinical observations of the ocular oncologist to the treatment planning.

Overall, small differences were observed between MRI-based and ultrasound-based height and LBD measurements of the tumor, which are in line with an earlier study.[15] However, we observed larger differences when the full tumor extent was not visible on ultrasound, which, in some of the patients, was attributed to the lower penetration depth of the ultrasound biomicroscopy probe (mean absolute difference reliable height measurements: 0.44 mm vs. unreliable: 0.76 mm and LBD: 1.15 mm vs. 1.67 mm). As MRI could be used to visualize the complete extent of the tumor and 3D reconstructions could be made regardless of the location of the tumor, MRI was considered more reliable for these tumors. Interestingly, the majority (14/20) of these unreliable measurements concerned anteriorly located tumors, and in 43% of these patients, the ophthalmologist already had doubts on the accuracy of the measurements during the ultrasound examination and had therefore requested MRI to be performed to confirm the measurements. Although in general the reproducibility of MRI-based measurements can be hampered by differences in window level settings between observers, we recently reported a 0.4-mm observer variation in MRI-based tumor delineation,[30] which is slightly better than the 0.6-mm to 0.7-mm variation reported for B-scan ultrasound.[31,32] Fundoscopic images can be used for measurement of the LBD of the tumor and gross tumor volume definition[4]; however, the optical aberrations present in these images can result in large, 1.2-mm differences compared with ultrasound,[33] making this technique less desirable to assess tumor dimensions. Nevertheless, a combined evaluation is certainly advised, especially for flat UM.

A	Markers	OR – MRI (mm)	
	N (%)	Mean (abs)	Largest
All markers	87 (100%)	-1.2 (2.0)	-13.9
<1 mm diff	48 (55%)		
>1 mm diff	39 (45%)		
Flat tumours	13 (15%)	-1.6 (5.2)	-13.9
Complex MT relation	13 (15%)	-3.0 (3.2)	-7.9
Shadow	9 (10%)	-3.7 (3.7)	-8.0
Interchanged annotation	4 (5%)	-0.6 (2.3)	-2.9

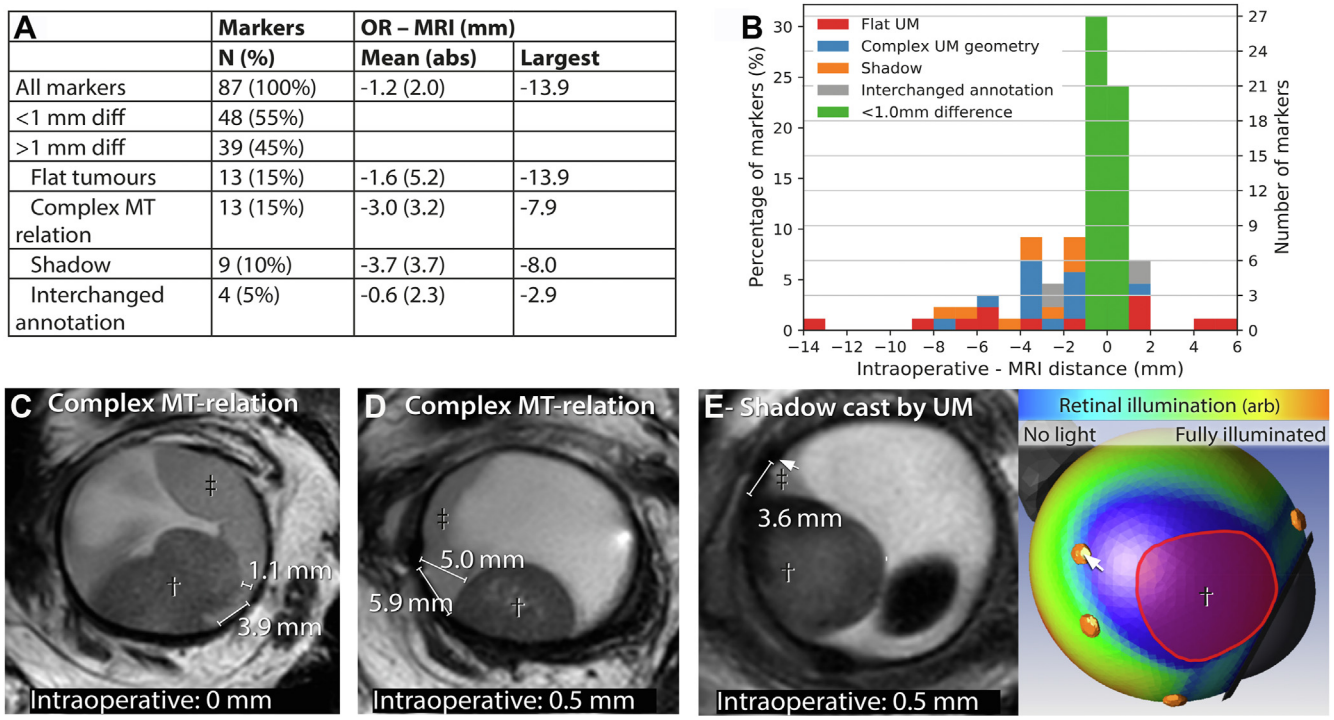

Figure 6. Intraoperative marker-tumor distances measurement compared with magnetic resonance imaging (MRI)-based measurements. A negative value means that the MRI distance was larger than the interoprative measurement. **A, B,** In 55% of the markers, a difference of < 1 mm was observed (green). The largest differences, up to 14 mm, were observed in flat melanoma (red). For 25% markers, the difference was attributed to a complex tumor geometry (blue) or shadow cast by the tumor (orange). **C, D,** For tumors with a complex marker-tumor relation, 1 length might not be sufficient to describe the marker-tumor relation. **E,** For anteriorly located tumors, the distance between posterior markers and tumor can be underestimated intraoperatively owing to a shadow that is cast by the tumor. abs = absolute; MT = marker-tumor; OR = ioperation room but reflects the intraoperative measurements; UM = uveal melanoma.

It should be noted that this cohort predominantly contained larger tumors, which often have a complex geometry, as the majority of smaller UM are treated with brachytherapy at our center. The results from this study can, therefore, not be generalized to the complete population of patients with UM, as the full extent of smaller tumors, for example, can generally be accurately visualized on ultrasound. In this context, ultrasound remains one of the principal modalities for the diagnosis for intraocular masses, as it is a less expensive, faster, and, for ophthalmologists, more accessible imaging modality than MRI.

In the majority (55%) of the patients, the MRI and intraoperative marker-tumor distances differed by <1.0 mm. For flat melanomas, the intraoperative marker-tumor distances were generally considered more reliable, as the edge of the flat parts of the tumor are difficult to determine with MRI, whereas they can be accurately be determined through transillumination in combination with fundoscopy. It is recognized in the field that, especially for more prominent anterior tumors, a surgeon can be misled by a penumbra during transpupillary transillumination.[34] Our results showed that the posterior extent of anteriorly located tumors can indeed be overestimated intraoperatively up to 8 mm, even when a combination of transpupillary transillumination and transocular transillumination is used. The amount of overestimation depends on multiple factors, including pupil diameter, tumor height, and presence of retinal detachment or hemorrhage. Therefore, for anteriorly located tumors, MRI can be considered a more reliable technique to determine the posterior extension of the tumor than the conventional optical techniques.

For both tumor height and marker-tumor distance measurements, differences between conventional and MRI-based measurements were, in some patients, attributed to a complex 3D geometry of the tumor, in which a different interpretation of the height and basal diameter was found between the radiologists and ophthalmologists. A more precise definition, incorporating how to evaluate complexly shaped tumors on 3D imaging, will likely aid in more uniform measurements and subsequent PT planning. However, these tumors clearly show that the conventional 1-dimensional measurements poorly describe the tumor geometry and relation to the markers. The different efforts working toward MRI-based ocular PT planning[35–37] will, therefore, likely enable a more precise incorporation of the tumor and marker relation.[14,28,29,35–38]

In 15 of 22 patients, the biometry showed signs of a potentially erroneous measurement due to the UM, explaining the large differences of up to 1.8 mm compared with MRI. For the patients with a reliable optical biometry measurement, however, a good agreement (<0.4 mm

difference) was found between MRI and biometry. This is similar to the 0.1-mm difference found in earlier studies with healthy eyes using automatic analysis of the MRI scans.[18,25] Moreover, MRI-based measurements of the axial length were found to be reproducible and a good alternative when biometry could be obtained reliably.[17] In the past, ultrasonic biometry has been used[4]; however, optical biometry has become the gold standard in ophthalmology owing to its higher accuracy and reproducibility, except for patients in whom optical evaluations are not possible, for example, in the case of a dense cataract or vitreous hemmorage.[39] Alternatively, using data from the contralateral eye has been proposed, as it is unaffected by intraocular pathologies. However, as eye lengths can differ between both eyes,[40] this can be less accurate than MRI-based measurements of the affected eye, as is further assessed in Appendix S1.

This study also showed some limitations in the MRI methods used. Similar to ultrasound, the extension of the (partially) flat UM could not always be determined reliably. Although MRI has a superior soft tissue contrast compared with ultrasound,[16,41] these flat UMs could not always be differentiated from the choroid. Second, in 2 patients, on MRI, a hemorrhagic or thickened and more enhancing choroid was observed directly adjacent to the tumor. Although this was not included as part of the tumor in both the basal diameter and marker-tumor measurements, histopathologic confirmation is needed for this interpretation. Finally, to improve the differentiation between tumor and retinal detachment, we started administering a contrast agent for the postoperative scans. It is therefore important to acknowledge these limitations of MRI and combine information from the different available sources to determine which measurement is the most reliable.

In the majority (20/23) of the patients included in this study, at least 1 of the measurements used for treatment planning of ocular PT was considered to be more reliable on MRI. Although the clinical implications of the inclusion of these MRI-based measurements on the final treatment plan need further evaluation, it is likely that MRI can reduce the uncertainties in ocular PT. Such a clinical evaluation should also consider the added costs of the MRI. Although health care costs vary greatly between countries, MRI is generally more expensive than ultrasound (e.g., ∼300€ and ∼100€, respectively, in the Netherlands).[42] However, the increased cost of including MRI is relative small compared with the costs of PT or costs associated with vision loss (10.000€−30.000€).[43,44] As a result, including MRI in the preparation for ocular PT is likely cost effective, as has been shown earlier in the context of treatment decision making.[45]

Although this study shows the benefit of including MRI in the planning for ocular PT, the importance of the ophthalmic evaluations should not be underestimated. As ophthalmic imaging data can contain information that is missed on MRI, such as the presence of a flat tumor extension, a combined evaluation of all available imaging data remains advised.

In conclusion, MRI provides valuable information for the planning of ocular PT, as it allows for a 3D assessment of the tumor and surrounding tissue. In specific cases, it provided more reliable measurements of axial length, tumor dimensions, and marker-tumor distances. Nevertheless, a combined evaluation, including ultrasound and optical imaging, remains advised, especially for flat UM.

Footnotes and Disclosures

Originally received: March 9, 2022.
Final revision: June 17, 2022.
Accepted: June 24, 2022.
Available online: July 13, 2022. Manuscript no. ORET-D-22-00175R2.

[1] Department of Ophthalmology, Leiden University Medical Center, Leiden, The Netherlands.

[2] Department of Radiology, Leiden University Medical Center, Leiden, The Netherlands.

[3] HollandPTC, Delft, The Netherlands.

[4] Department of Radiation Oncology, Leiden University Medical Center, Leiden, The Netherlands.

Disclosure(s):

All authors have completed and submitted the ICMJE disclosures form.

The author(s) have made the following disclosure(s): T.A.F.: Support − Protons4VISION (Netherlands Organization for Scientific Research, NWO; project number 14654), Dutch Cancer Society (KWF; project number 2019: 12184).

B.M.V.: Research grant − Varian.

J.-W.M.B.: Support − Netherlands Organization for Scientific Research (NWO; Protons4VISION 14654); Research support − Philips Healthcare; Leadership or fiduciary role − Chair pathology and oncology section of European Vision and Eye Research Society.

The other authors have no proprietary or commercial interest in any materials discussed in this article.

Supported by Philips Healthcare. They had no role in the design of the study; collection, analyses, and interpretation of data; writing of the manuscript, and decision to publish the results.

Funded by the Netherlands Organisation for Scientific Research (NWO; Protons4VISION 14654).

HUMAN SUBJECTS: Human subjects were included in this study. The study was approved by the Ethics Committee METC Leiden Den Haag Delft (G20.16; January 4, 2021). All research adhered to the tenets of the Declaration of Helsinki. All participants provided informed consent.

No animal subjects were used in this study.

Author Contributions:

Conception and design: Jaarsma-Coes, Beenakker

Data collection: Jaarsma-Coes, Ferreira, Marinkovic, Vu, Vught, Haren, Rodrigues, Klaver, Verbist, Luyten, Rasch, Beenakker

Analysis and interpretation: Jaarsma-Coes, Ferreira, Marinkovic, Vu, Vught, Verbist, Luyten, Rasch, Beenakker

Obtained funding: Luyten, Beenakker; tudy was performed as part of the authors' regular employment duties. No additional funding was provided.

Overall responsibility: Jaarsma-Coes, Ferreira, Marinkovic, Vu, Vught, Haren, Rodrigues, Klaver, Verbist, Luyten, Rasch, Beenakker

Abbreviations and Acronyms:
2D = 2-dimensional; **3D** = 3-dimensional; **IQR** = interquartile range; **LBD** = largest basal diameter; **MRI** = magnetic resonance imaging; **PT** = proton therapy; **UM** = uveal melanoma.

Keywords:
Magnetic resonance imaging, Ocular oncology, Proton beam therapy, Ultrasound, Uveal melanoma.

Correspondence:
Jan-Willem M. Beenakker, PhD, Albinusdreef 22333ZA Leiden, The Netherlands. E-mail: j.w.m.beenakker@lumc.nl.

References

1. Aronow ME, Topham AK, Singh AD. Uveal melanoma: 5-year update on incidence, treatment, and survival (SEER 1973-2013). *Ocul Oncol Pathol*. 2018;4:145−151.
2. IKNL. NKR cijfers. https://iknl.nl/nkr-cijfers. Accessed March 23, 2022.
3. Mishra KK, Daftari IK. Proton therapy for the management of uveal melanoma and other ocular tumors. *Chin Clin Oncol*. 2016;5:50.
4. Hrbacek J, Mishra KK, Kacperek A, et al. Practice patterns analysis of ocular proton therapy centers: the international OPTIC survey. *Int J Radiat Oncol Biol Phys*. 2016;95:336−343.
5. Egger E, Schalenbourg A, Zografos L, et al. Maximizing local tumor control and survival after proton beam radiotherapy of uveal melanoma. *Int J Radiat Oncol Biol Phys*. 2001;51:138−147.
6. Damato B, Kacperek A, Chopra M, et al. Proton beam radiotherapy of choroidal melanoma: the Liverpool-Clatterbridge experience. *Int J Radiat Oncol Biol Phys*. 2005;62:1405−1411.
7. Papakostas TD, Lane AM, Morrison M, et al. Long-term outcomes after proton beam irradiation in patients with large choroidal melanomas. *JAMA Ophthalmol*. 2017;135:1191−1196.
8. Sikuade MJ, Salvi S, Rundle PA, et al. Outcomes of treatment with stereotactic radiosurgery or proton beam therapy for choroidal melanoma. *Eye (Lond)*. 2015;29:1194−1198.
9. Russo A, Mariotti C, Longo A, et al. Diffusion-weighted magnetic resonance imaging and ultrasound evaluation of choroidal melanomas after proton-beam therapy. *Radiol Med*. 2015;120:634−640.
10. Ferreira TA, Fonk LG, Jaarsma-Coes MG, et al. MRI of uveal melanoma. *Cancers (Basel)*. 2019;11:1−20.
11. Niendorf T, Beenakker JWM, Langner S, et al. Ophthalmic magnetic resonance imaging: where are we (heading to)? *Curr Eye Res*. 2021;46:1251−1270.
12. Beenakker JWM, Brouwer NJ, Chau C, et al. Outcome measures of new technologies in uveal melanoma: review from the European vision institute special interest focus group meeting. *Ophthalmic Res*. In press. doi: 10.1159/000524372
13. Fleury E, Trnková P, van Rij C, et al. Improving organs-at-risk sparing for choroidal melanoma patients: a CT-based two-beam strategy in ocular proton therapy with a dedicated eye-line. *Radiother Oncol*. 2022;171:173−181.
14. Hassan MK, Fleury E, Shamonin D, et al. An automatic framework to create patient-specific eye models from 3D magnetic resonance images for treatment selection in patients with uveal melanoma. *Adv Radiat Oncol*. 2021;6:100697.
15. Ferreira TA, Jaarma-Coes MG, Marinkovic M, et al. MR imaging characteristics of uveal melanoma with histopathological validation. *Neuroradiology*. 2022;64:171−184.
16. Beenakker JWM, Ferreira TA, Soemarwoto KP, et al. Clinical evaluation of ultra-high-field MRI for three-dimensional visualisation of tumour size in uveal melanoma patients, with direct relevance to treatment planning. *MAGMA*. 2016;29:571−577.
17. Wiseman SJ, Tatham AJ, Meijboom R, et al. Measuring axial length of the eye from magnetic resonance brain imaging. *BMC Ophthalmol*. 2022;22:54.
18. van Vught L, Shamonin DP, Luyten GPM, et al. MRI-based 3D retinal shape determination. *BMJ Open Ophthalmol*. 2021;6. e000855−e000855.
19. Oberacker E, Paul K, Huelnhagen T, et al. Magnetic resonance safety and compatibility of tantalum markers used in proton beam therapy for intraocular tumors: a 7.0 Tesla study. *Magn Reson Med*. 2017;78:1533−1546.
20. Bergman L, Nilsson B, Lundell G, et al. Ruthenium brachytherapy for uveal melanoma, 1979−2003: survival and functional outcomes in the Swedish population. *Ophthalmology*. 2005;112:834−840.
21. Marinkovic M, Horeweg N, Fiocco M, et al. Ruthenium-106 brachytherapy for choroidal melanoma without transpupillary thermotherapy: similar efficacy with improved visual outcome. *Eur J Cancer*. 2016;68:106−113.
22. Haag-Streit Diagnostics. Instructions for use Biometer Lenstar LS 900. 2014:24. https://www.doctor-hill.com/physicians/docs/Lenstar-User-Manual.pdf. Accessed February 26, 2021.
23. van Vught L, Dekker CE, Stoel BC, et al. Evaluation of intraocular lens position and retinal shape in negative dysphotopsia using high-resolution magnetic resonance imaging. *J Cataract Refract Surg*. 2021;47:1032−1038.
24. van Vught L, Luyten GPM, Beenakker JWM. Distinct differences in anterior chamber configuration and peripheral aberrations in negative dysphotopsia. *J Cataract Refract Surg*. 2020;46:1007−1015.
25. Beenakker JWM, Shamonin DP, Webb AG, et al. Automated retinal topographic maps measured with magnetic resonance imaging. *Invest Ophthalmol Vis Sci*. 2015;56:1033−1039.
26. Baron ED, Di Nicola M, Shields CL. Updated AJCC classification for posterior uveal melanoma: a case example of a patient with choroidal melanoma is discussed in light of the latest edition of this cancer staging manual. *Retin Today*. 2018:30−34.
27. Daftari Ik, Aghaian E, O'Brien JM, et al. 3D MRI-based tumor delineation of ocular melanoma and its comparison with conventional techniques. *Med Phys*. 2005;32:3355−3362.
28. Marnitz S, Cordini D, Bendl R, et al. Proton therapy of uveal melanomas: intercomparison of MRI-based and conventional treatment planning. *Strahlenther Onkol*. 2006;182:395−399.
29. Via R, Hennings F, Pica A, et al. Potential and pitfalls of 1.5T MRI imaging for target volume definition in ocular proton therapy. *Radiother Oncol*. 2021;154:53−59.
30. Jaarsma-Coes MG, Klaassen L, Verbis BM, et al. Inter-observer variability in MR-based target volume delineation of uveal melanoma, unpublished data, 2022
31. Char DH, Kroll S, Stone RD, et al. Ultrasonographic measurement of uveal melanoma thickness: interobserver variability. *Br J Ophthalmol*. 1990;74:183−185.
32. Haritoglou C, Neubauer AS, Herzum H, et al. Interobserver and intraobserver variability of measurements of uveal melanomas using standardised echography. *Br J Ophthalmol*. 2002;86:1390−1394.
33. Pe'er JJ, Sancho C, Cantu J, et al. Measuring choroidal melanoma basal diameter: using ultrasound vs. a new wide−angle fundus camera. *Invest Ophthalmol Vis Sci*. 2004;45:1223.
34. Damato B, Kacperek A, Errington D, Heimann H. Proton beam radiotherapy of uveal melanoma. *Saudi J Ophthalmol*. 2013;27:151−157.
35. Fleury E, Trnková P, Erdal E, et al. Three-dimensional MRI-based treatment planning approach for non-invasive ocular proton therapy. *Med Phys*. 2021;48:1315−1326.

36. Pfeiffer K, Dobler B, Rethfeldt C, et al. OCTOPUS: a planning tool for proton therapy of eye tumours. In: Schlegel W, Bortfeld T, eds. *The Use of Computers in Radiation Therapy*. Berlin, Heidelberg: Springer; 2000.
37. Nguyen HG, Pica A, Hrbacek J, et al. A novel segmentation framework for uveal melanoma in magnetic resonance imaging based on class activation maps. *Proc Mach Learn Res*. 2019;102:370–379.
38. Nguyen HG, Sznitman R, Maeder P, et al. Personalized anatomic eye model from T1-weighted volume interpolated gradient echo magnetic resonance imaging of patients with uveal melanoma. *Int J Radiat Oncol Biol Phys*. 2018;102:813–820.
39. Kane JX, Chang DF. Intraocular lens power formulas, biometry, and intraoperative aberrometry: a review. *Ophthalmology*. 2021;128:e94–e114.
40. Rajan MS, Bunce C, Tuft S. Interocular axial length difference and age-related cataract. *J Cataract Refract Surg*. 2008;34:76–79.
41. Afonso P, Mascarenhas V. Imaging techniques for the diagnosis of soft tissue tumors. *Reports Med Imaging*. 2015;201:63–70.
42. Nederlandse Zorgautoriteit. Tarieventabel dbc-zorgproducten en overige-zorgproducten per 1 januari 2019. PUC_236092_22 2019. https://puc.overheid.nl/nza/doc/PUC_236092_22/1/. Accessed June 17, 2022.
43. Moriarty JP, Borah BJ, Foote RL, et al. Cost-effectiveness of proton beam therapy for intraocular melanoma. *PLoS One*. 2015;10:e0127814.
44. Köberlein J, Beifus K, Schaffert C, Finger RP. The economic burden of visual impairment and blindness: a systematic review. *BMJ Open*. 2013;3:e003471.
45. Fonk LG, Ferreira TA, Webb AG, et al. The economic value of MR-imaging for uveal melanoma. *Clin Ophthalmol*. 2020;14:1135–1143.

Pictures & Perspectives

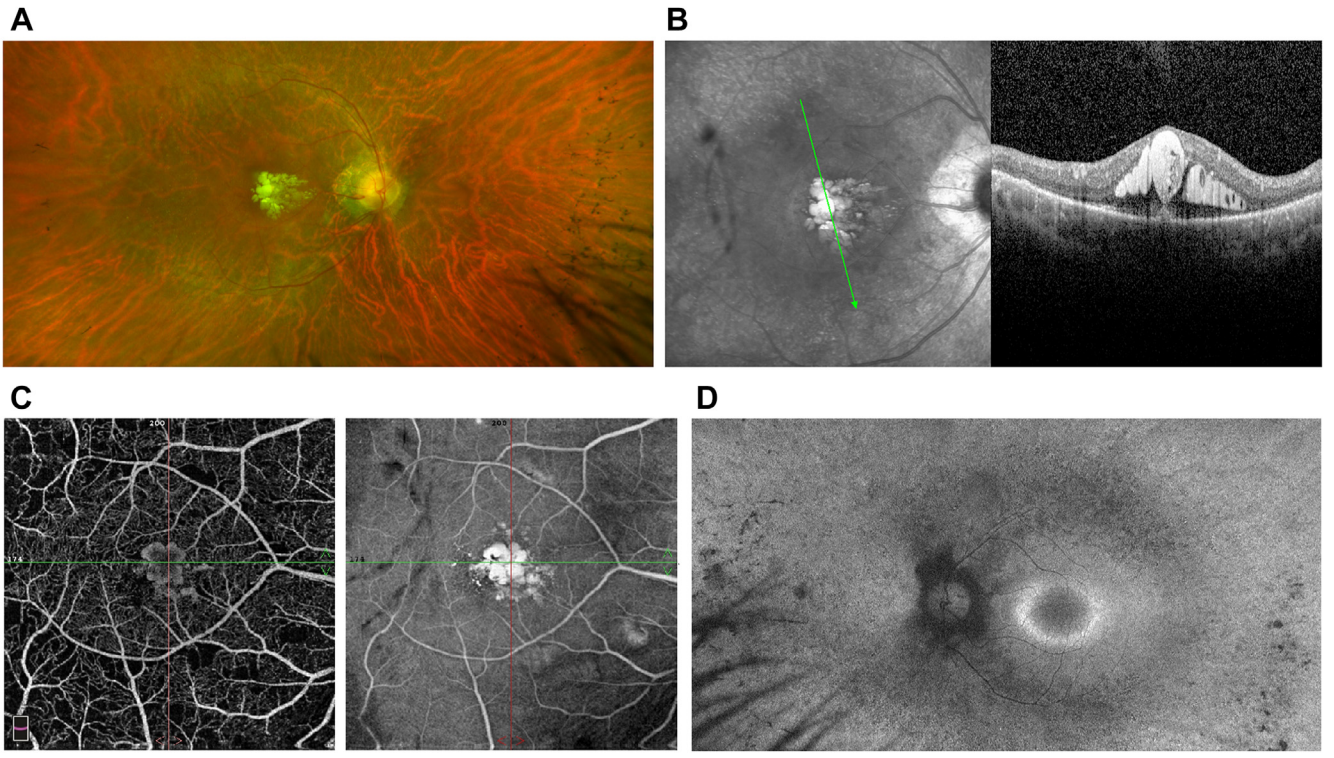

"Lipoid" Macular Edema in Familial Hypertriglyceridemia and Retinal Dystrophy

A 45-year-old man presented with decreased vision in the right eye. Relevant medical history included familial hypertriglyceridemia, kidney transplantation, sensorineural hearing loss, and diabetes. Fundoscopy revealed yellowish petaloid-shaped intraretinal deposits, along with vessel attenuation and bone spicule hyperpigmentation in the midperiphery (Fig **A**). On spectral-domain–OCT, cystoid cavities filled with a hyperreflective material were noted, presumably because of elevated serum triglyceride levels (4615 mg/dL) (Fig **B**). There were no signs of diabetic retinopathy on OCT angiography (Fig **C**). On fundus autofluorescence, a parafoveal hyperautofluorescent ring was present bilaterally (Fig **D**). This is a rare case of hyperreflective cystoid macular edema presumably associated with hypertriglyceridemia in a patient with probable Senior-Løken syndrome. (Magnified version of Fig **A-D** is available online at www.ophthalmologyretina.org).

Rosa Lomelino Pinheiro, MD[1]
João Pedro Marques, MD, MSc[1,2,3]
Joaquim Neto Murta, MD, PhD[1,2,3]

[1]Centro de Responsabilidade Integrado de Oftalmologia, Centro Hospitalar e Universitário de Coimbra, Coimbra, Portugal; [2]Clinical Academic Center of Coimbra (CACC), Coimbra, Portugal; [3]Faculty of Medicine, University of Coimbra, Coimbra, Portugal